

The CREB1 inhibitor 666-15 maintains cartilage homeostasis and mitigates osteoarthritis progression

Cite this article:

Bone Joint Res 2024;13(1):
4–18.

DOI: 10.1302/2046-3758.
131.BJR-2023-0016.R2

Correspondence should be
sent to Chengai Wu
wuchengai@jst-hosp.com.cn

Y. Wang,¹ Z. Wu,¹ G. Yan,² S. Li,¹ Y. Zhang,¹ G. Li,³ C. Wu¹

¹Department of Molecular Orthopedics, National Center for Orthopaedics, Beijing Research Institute of Traumatology and Orthopaedics, Beijing Jishuitan Hospital, Capital Medical University, Beijing, China

²National Center for Orthopaedics, Animal Laboratory, Beijing Research Institute of Traumatology and Orthopaedics, Beijing Jishuitan Hospital, Capital Medical University, Beijing, China

³National Center for Orthopaedics, Laboratory of Bone Tissue Engineering, Beijing Research Institute of Traumatology and Orthopaedics, Beijing Jishuitan Hospital, Capital Medical University, Beijing, China

Aims

cAMP response element binding protein (CREB1) is involved in the progression of osteoarthritis (OA). However, available findings about the role of CREB1 in OA are inconsistent. 666-15 is a potent and selective CREB1 inhibitor, but its role in OA is unclear. This study aimed to investigate the precise role of CREB1 in OA, and whether 666-15 exerts an anti-OA effect.

Methods

CREB1 activity and expression of a disintegrin and metalloproteinase with thrombospondin motifs 4 (ADAMTS4) in cells and tissues were measured by immunoblotting and immunohistochemical (IHC) staining. The effect of 666-15 on chondrocyte viability and apoptosis was examined by cell counting kit-8 (CCK-8) assay, JC-10, and terminal deoxynucleotidyl transferase-mediated dUTP nick end-labelling (TUNEL) staining. The effect of 666-15 on the microstructure of subchondral bone, and the synthesis and catabolism of cartilage, in anterior cruciate ligament transection mice were detected by micro-CT, safranin O and fast green (S/F), immunohistochemical staining, and enzyme-linked immunosorbent assay (ELISA).

Results

CREB1 was hyperactive in osteoarthritic articular cartilage, interleukin (IL)-1 β -treated cartilage explants, and IL-1 β - or carbonyl cyanide 3-chlorophenylhydrazide (CCCP)-treated chondrocytes. 666-15 enhanced cell viability of OA-like chondrocytes and alleviated IL-1 β - or CCCP-induced chondrocyte injury through inhibition of mitochondrial dysfunction-associated apoptosis. Moreover, inhibition of CREB1 by 666-15 suppressed expression of ADAMTS4. Additionally, 666-15 alleviated joint degeneration in an ACLT mouse model.

Conclusion

Hyperactive CREB1 played a critical role in OA development, and 666-15 exerted anti-IL-1 β or anti-CCCP effects *in vitro* as well as joint-protective effects *in vivo*. 666-15 may therefore be used as a promising anti-OA drug.

Article focus

- Studies on the role of CREB1 in the pathogenesis of osteoarthritis (OA) yield inconsistent results. Hence, the exact role of CREB1 in OA needs to be further explored.
- 666-15 is a potent and selective CREB1 inhibitor that exerts anti-tumour effects. However, the role of 666-15 in OA remains unclear.

Key messages

- CREB1 was hyperactive in osteoarthritic articular cartilage *in vivo*, cartilage explant *ex vivo*, and chondrocytes *in vitro*.
- CREB1 inhibition by 666-15 enhanced viability of OA-like chondrocytes, and alleviated IL-1 β - or carbonyl cyanide 3-chlorophenylhydrazone (CCCP)-induced chondrocyte injury through inhibition of mitochondrial dysfunction-associated apoptosis.
- 666-15 alleviated joint degeneration in an anterior cruciate ligament transection mouse model.

Strengths and limitations

- To our knowledge, this is the first time that the therapeutic potential of 666-15 in diminishing OA deterioration has been highlighted. These findings unveiled 666-15 as a promising anti-OA drug.
- It is unfortunate that we were unable to verify the therapeutic effect of 666-15 in human OA.

Introduction

Osteoarthritis (OA) is the most common degenerative joint disorder, affecting largely the knees and hips, and is characterized by increasing loss of cartilage, subchondral bone remodelling, and inflammation in the synovial membrane.¹ To date, the pathogenesis of OA remains enigmatic, and identification of the principal molecular mechanisms underlying the initiation and progression of OA is urgently needed. Depending on the stage of the disease, current treatment strategies constitute chronic pain relief and joint mobility preservation by viscosupplementation injection or physiotherapy for early-stage OA,² as well as total joint replacement surgery for end-stage OA.³ However, there is still a lack of disease-modifying OA drugs or agents that may improve joint homeostasis.² A substantial amount of time and effort is required to investigate potential therapeutic drugs that may alter the degenerated joint phenotype in OA.

Although OA affects all anatomical components of the joint, the degradation of articular cartilage is the pathological hallmark of OA. Articular cartilage is a type of highly organized avascular fibrous connective tissue that functions as a shock absorber with low-friction and low-wear properties, as well as providing smooth articulation at the joint surfaces.^{4,5} It is composed of a complex extracellular matrix (ECM) largely comprising type II collagen and aggrecan, a large aggregating chondroitin-sulfate proteoglycan, as well as sparse specialized cells called chondrocytes.⁶ As the sole cell population in cartilage, chondrocytes play a significant role in the development and maintenance of ECM, which is in a dynamic state of equilibrium between synthesis and degradation.^{7,8} Matrix metalloproteinase 13 (MMP13) and a disintegrin and metalloproteinase with thrombospondin motifs 4 (ADAMTS4) are considered the most critical ECM catabolic enzymes

associated with the degradation of collagen and aggrecan, respectively, in OA.^{9,10} Dysregulation of these ECM-degrading enzymes can disturb the balance between synthesis and degradation of ECM, and can lead to progressively pathological destruction in cartilage.¹¹

cAMP response element binding protein (CREB1) is a nuclear transcription factor that regulates cell survival and cell death.¹² Activation of CREB1, dependent on phosphorylation at Ser133 by several kinases,¹³ is implicated in various pathologies.¹⁴⁻¹⁶ The role of CREB1 in the pathogenesis of OA has drawn more attention in recent years. Using bioinformatics tools, CREB1 has been identified as one of the crucial transcriptional factors in the regulatory network of OA.¹⁷ CREB1 induces MMP13 expression following a specific CpG demethylation in osteoarthritic cartilage.¹⁸ Activation of the p38/CREB/MMP13 axis has also been reported in hip OA.¹⁹ However, CREB1 appears to have the ability to promote chondrocyte proliferation, as downregulation of CREB1 results in inhibition of chondrocyte proliferation.²⁰ Thus, the effects of CREB1 on cartilage remain inconclusive, and whether targeting CREB1 is a promising therapeutic strategy for OA needs to be determined.

666-15 is a potent and selective CREB1 inhibitor that decreases CREB1 activation.^{21,22} It has been reported that 666-15 shows efficacious antitumour activity *in vivo*.^{23,24} However, whether 666-15 promotes chondroprotective activities and anti-osteoarthritic effects is uncertain.

In the present study, we aimed to address: 1) whether CREB1 in cartilage from osteoarthritic animal or cell models is hyperactive; and 2) whether 666-15, a potent CREB1 inhibitor, maintains cartilage homeostasis and mitigates OA progression.

Methods

Reagents and antibodies

666-15 was procured from AbMole Bioscience (USA). Human and mouse IL-1 β were obtained from Novoprotein (China). Carbonyl cyanide 3-chlorophenylhydrazone (CCCP) was from Solarbio (China). Hoechst 33,258 was from Biorigin (China). DMEM-low glucose (LG) and fetal bovine serum (FBS) were from HyClone (USA). Anti-p-CREB1 was purchased from Cell Signaling Technology (USA). Antibodies against aggrecan, ADAMTS4, and β -actin were obtained from Abcam (USA). Antibodies against collagen II and MMP13 were purchased from Proteintech (USA). Horseradish peroxidase (HRP)-labelled goat anti-mouse and HRP-labelled goat anti-rabbit antibodies were from Applygen (China) and Cell Signaling Technology (USA).

Animals

Both Hartley guinea pigs ($n = 18$, one-month-old, female) and C57BL/6 N mice ($n = 37$, six-week-old, male) were housed at 22°C ($\pm 2^\circ\text{C}$) with a relative humidity of 55% ($\pm 10\%$) and 12-hour light-dark cycle. The animals were given *ad libitum* access to water and standard rodent chow. All procedures of the animal experiments were approved and performed in accordance with the institutional guidelines for care and use of animals. All efforts were made to minimize the number of animals killed in the experiment and their discomfort. Moreover, we have adhered to the ARRIVE guidelines and have supplied the relevant checklist.

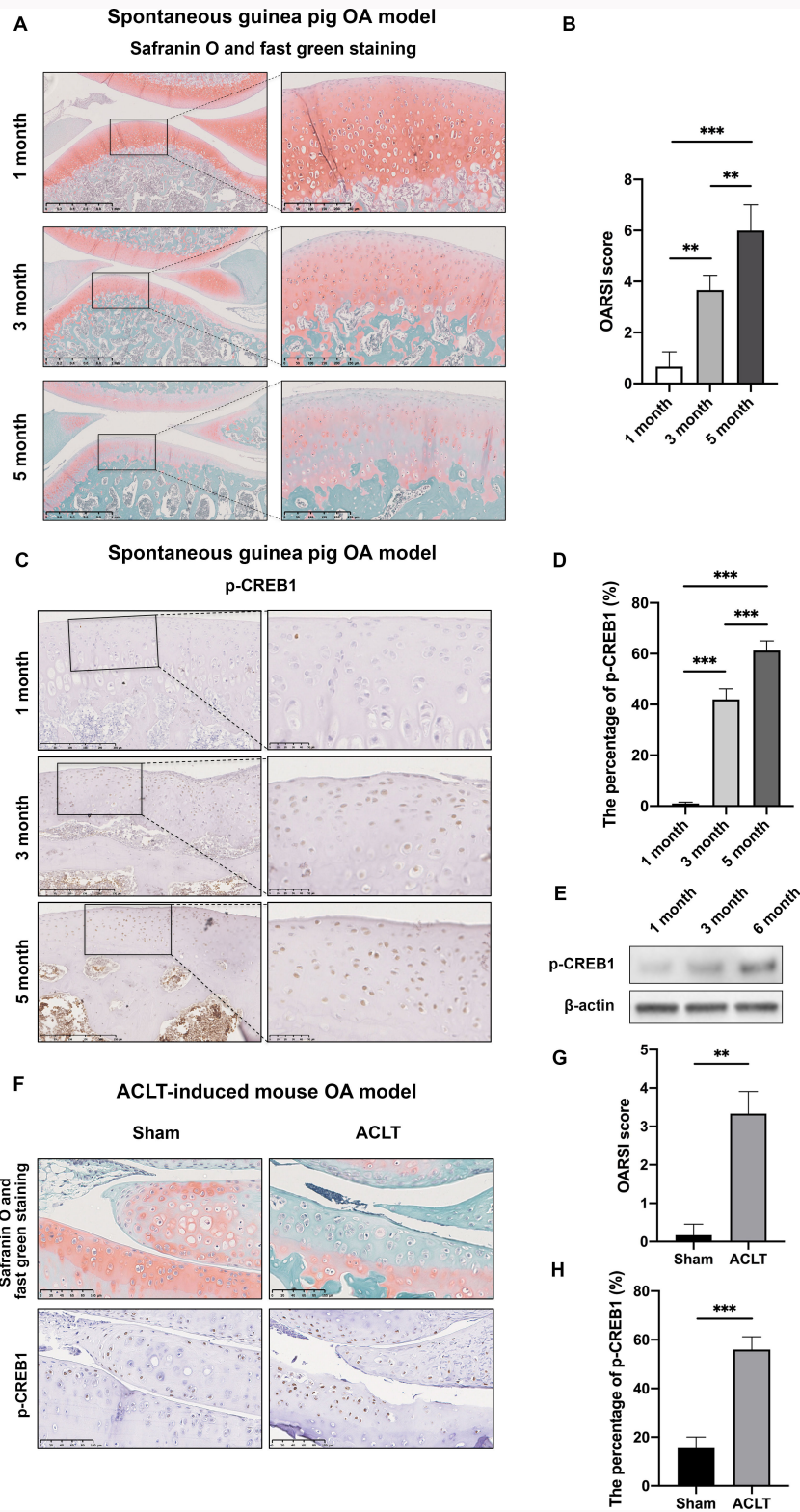


Fig. 1

cAMP response element binding protein (CREB1) was activated in the degenerative cartilage in both spontaneous and instability-induced osteoarthritis (OA) models in vivo. a) Safranin O and fast green (S/F) staining of articular cartilage in sagittal sections of the tibia from guinea pigs of different ages (left panel, scale bars = 1 mm; right panel, scale bars = 250 μ m). b) The Osteoarthritis Research Society International (OARSIS) scores of histological sections of the tibia from guinea pigs of different ages (n = 3 in each group). c) Levels of p-CREB1 in the articular cartilage increased gradually with age. Representative images are shown of immunohistochemistry (IHC) with antibody against p-CREB1 in the articular cartilage of guinea pigs of different ages (left panel, scale bars = 250 μ m; right panel, scale bars = 50 μ m). d) Quantitative analysis of the percentages of p-CREB1-positive chondrocytes in articular cartilage tissue sections in each group (n = 3 in each group). e) Levels of phosphorylation of CREB1 in primary chondrocytes derived from guinea pigs of different ages were determined by immunoblotting. f) to h) S/F staining and IHC staining of p-CREB1 in tibial cartilage of sham or anterior cruciate ligament transection (ACLT) mice (scale bars = 100 μ m), with f) representative images, g) OARSIS scores, and h) quantification of p-CREB1-positive chondrocytes of the tibial cartilage shown (n = 3 in each group). For b) and d), one-way analysis of variance was used to compare means among groups, and the Fisher's least significant difference test was performed for the multiple comparisons. For g) and h), the independent-samples *t*-test was used for comparisons between two groups. ***p* < 0.01, ****p* < 0.001, *****p* < 0.0001.

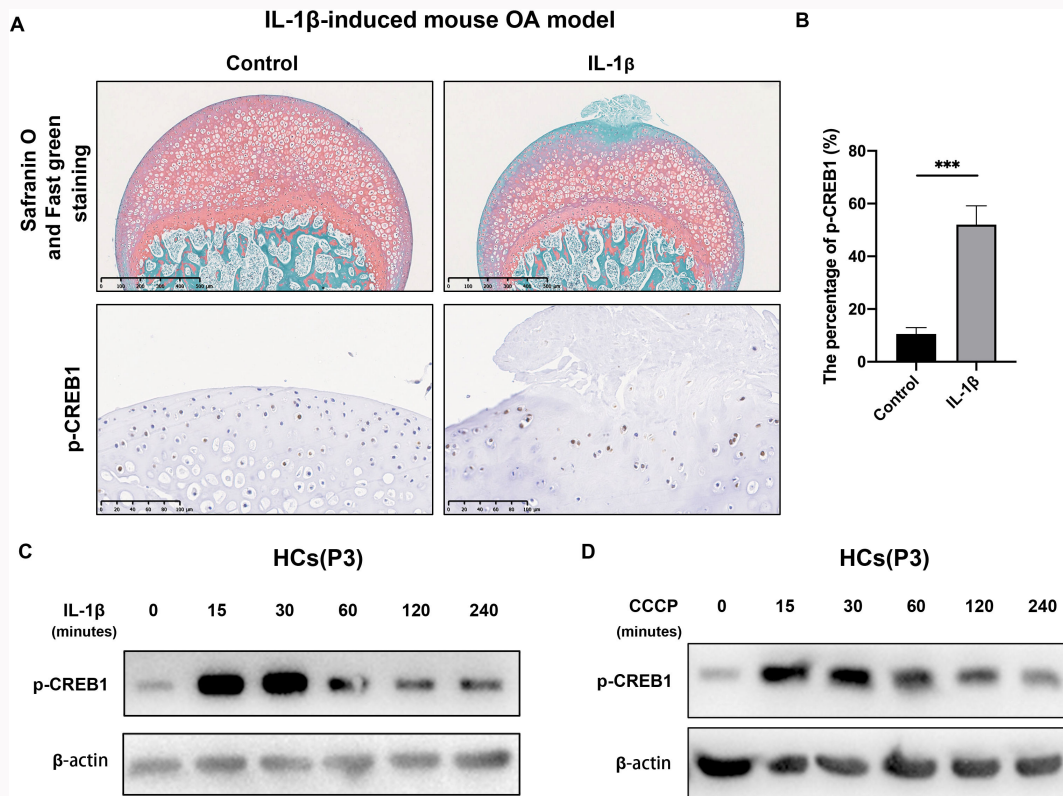


Fig. 2 cAMP response element binding protein (CREB1) was activated in osteoarthritic cartilage explants ex vivo and chondrocytes in vitro. a) Safranin O and fast green (S/F) staining (top panel, scale bars = 500 μ m) and immunohistochemical (IHC) staining of p-CREB1 (bottom panel, scale bars = 100 μ m) in cartilage of mouse femoral head treated with or without interleukin-1 β (IL-1 β) (10 ng/ml) for 72 hours. b) Quantification of IHC data (n = 3 in each group). The independent-samples *t*-test was used for comparisons between two groups; ***p < 0.001. c) to d) Human chondrocytes (HCs) of passage 3 (P3) were treated with c) IL-1 β (10 ng/ml) or d) carbonyl cyanide 3-chlorophenylhydrazone (CCCP) (50 μ M) for the indicated durations, and phosphorylation of CREB1 was determined by immunoblotting.

Spontaneous OA model

Guinea pigs were killed by cervical dislocation under anaesthesia using 3% sodium pentobarbital (30 mg/kg) via intraperitoneal injection at one, three, or five months of age (n = 3/group). Left knee joint specimens were collected and subjected to histological analysis.

Induction of knee post-traumatic OA

The anterior cruciate ligament transection (ACLT)-induced OA of the left knee was established according to previous research.^{25,26} In brief, after two weeks of acclimatization, ACLT was performed on the left knee joints of mice that had been anaesthetized with dexmedetomidine (0.25 mg/kg) and ketamine (25 mg/kg) by intramuscular injection. A sham operation was done on the left knee joints of mice without ACLT.

Experimental design for the established post-traumatic OA model

In this study, we performed two experiments for different purposes. In the first experiment, six mice were randomly assigned to the sham and ACLT groups (n = 3/group). The animals were killed six weeks after surgery, and knee joint samples were collected for histological examination of changes in degeneration and CREB1 activity in the knee joint cartilage. In the second experiment, a total of 25 mice were randomly assigned to normal, sham, ACLT + vehicle, ACLT +

666-15 low, and ACLT + 666-15 high groups (n = 5/group). Two weeks after surgery, the ACLT mice were injected intraperitoneally with either vehicle, 666-15 at 5 mg/kg, or 666-15 at 10 mg/kg once a week, and the treatment lasted for six weeks. 666-15 was dissolved in 10% dimethyl sulfoxide (DMSO), 40% polyethylene glycol (PEG 300), and 5% Tween-80 in saline. The 666-15 treatments were freshly prepared weekly. Both normal and sham group animals did not receive an injection. All mice were killed eight weeks post-surgery under anaesthesia with 0.25 mg/kg dexmedetomidine and 25 mg/kg ketamine by intramuscular injection. Blood samples and left knee joint specimens were harvested for subsequent experiments, including micro-CT analysis, histological analysis, immunohistochemistry (IHC) assessment, and enzyme-linked immunosorbent assay (ELISA).

Cartilage, chondrocytes, and drug treatment

Femoral heads from six-week-old, male C57BL/6 N mice were dissected and used as explants for ex vitro studies. Briefly, after stabilization in Dulbecco's Modified Eagle Medium Low Glucose (DMEM-LG) complete medium (DMEM-LG supplemented with 10% FBS, 100 U/ml penicillin, 100 μ g/ml streptomycin, and 250 ng/ml Amphotericin B) for 24 hours, femoral head explants were maintained in DMEM-LG complete medium with or without 10 ng/ml IL-1 β (n = 3/group) for another 72 hours. Afterward, femoral head explants with or

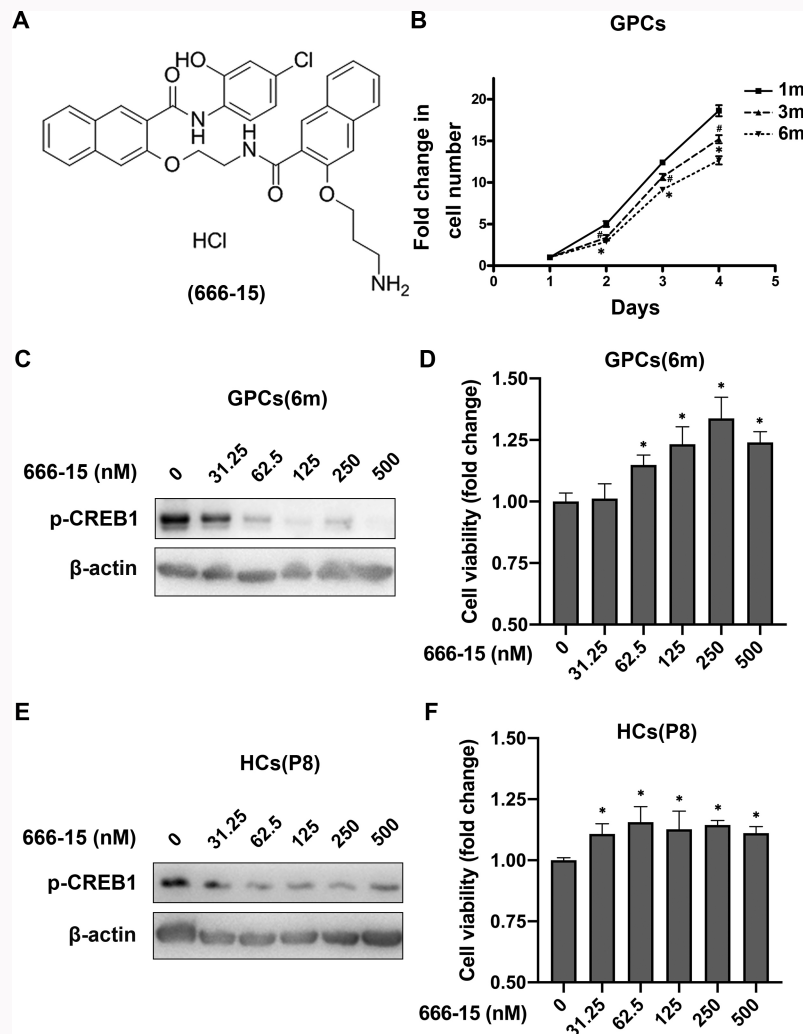


Fig. 3

666-15 suppressed cAMP response element binding protein (CREB1) activity and enhanced cell viability of aged chondrocytes in vitro. a) Chemical structure of 666-15. b) Viability of chondrocytes declined gradually with age. Cell viability of articular chondrocytes obtained from the knees of guinea pigs of different ages (1 m, 1 months; 3 m, 3 months; and 6 m, 6 months) ($n = 3$ in each group) was determined by cell counting kit-8 (CCK-8) assay. For each time point detected, one-way analysis of variance (ANOVA) was used to compare means among groups and the Fisher's least significant difference (LSD) test was performed for the multiple comparisons. # $p < 0.05$, 3 m vs 1 m; * $p < 0.05$, 6 m vs 1 m. c) to d) Chondrocytes obtained from six-month-old guinea pigs (GPCs (6 m)) were treated with different concentrations of 666-15 for 24 hours. Cell lysates were collected and c) subjected to immunoblotting to detect the phosphorylation level of CREB1, and d) CCK-8 assay was applied to detect cell viability ($n = 3$ in each group), one-way ANOVA was used to compare means among groups, and the Fisher's LSD test was performed for the multiple comparisons. * $p < 0.05$, vs vehicle group. e) to f) Human chondrocytes (HCs) of P8 were treated with different concentrations of 666-15 for 24 hours. e) Cells were harvested for protein extraction and immunoblotting, and f) cell viability was assessed by CCK-8 assay ($n = 3$ in each group), one-way ANOVA was used to compare means among groups, and the Fisher's LSD test was performed for the multiple comparisons. * $p < 0.05$, vs vehicle group. HCl, hydrogen chloride.

without OA-like defects were collected for histological analysis and IHC assessment. Human primary chondrocytes and their culture system were obtained from BeNa culture collection (BNCC, China). Different passages of human primary chondrocytes were used for different purposes in the study. To obtain the primary chondrocytes from animals of different ages at the same time, one-month-old guinea pigs were purchased and were maintained for zero, two, or five months, respectively. Knee joint articular cartilage from animals aged one, three, or six months ($n = 3$ /group) were harvested and subjected to sequential enzymatic digestion with trypsin and collagenase II under sterile conditions. Thereafter, isolated chondrocytes were collected and resuspended in DMEM-LG complete medium. Guinea pig chondrocytes between passages 2 and 5 were

used for experiments. All cartilage explants and cells were incubated in a humidified atmosphere of 5% CO_2 at 37°C. To induce OA-like changes in chondrocytes, cells were stimulated with 10 ng/ml IL-1 β or 50 μM CCCP at the designated time. To inhibit CREB1 activity, chondrocytes were treated with different concentrations of 666-15 for indicated time.

Micro-CT analysis of subchondral bone

Micro-CT analysis was performed as previously described.¹ Briefly, the microarchitecture of the knee joint samples was acquired on a SkyScan 1172 μCT system (Bruker Corporation, USA) operating at a source voltage of 49 kV and current of 139 μA with an image pixel size of 7.97 μm . For analysis of the subchondral bone, the compartment of the

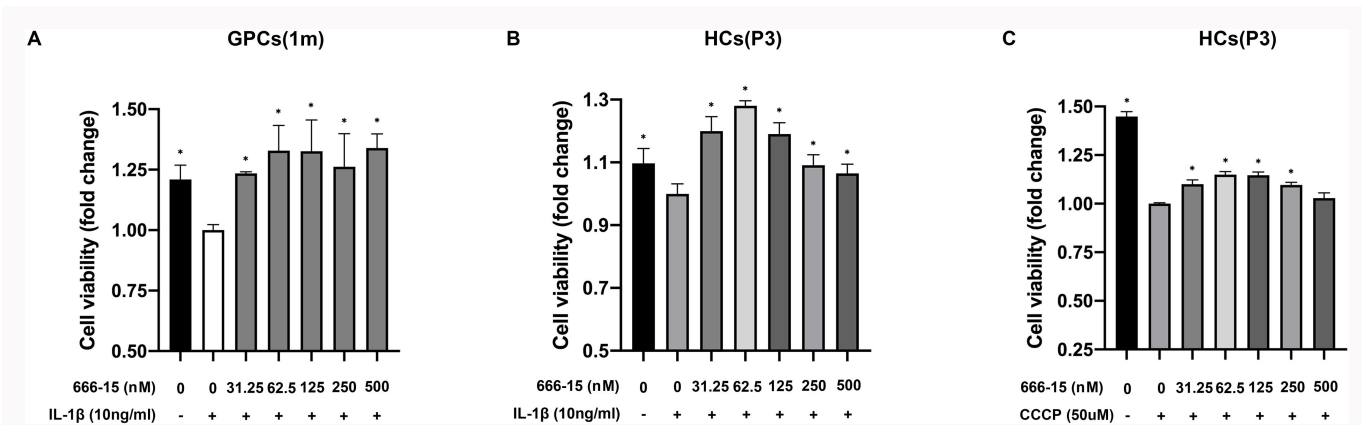


Fig. 4

666-15 alleviated IL-1 β - or carbonyl cyanide 3-chlorophenylhydrazone (CCCP)-induced chondrocyte injury through inhibition of mitochondrial dysfunction-associated apoptosis. a) Chondrocytes obtained from one-month-old guinea pigs (GPCs (1 m)) (n = 3 in each group) were treated with different concentrations of 666-15 for two hours prior to IL-1 β (10 ng/ml) treatment for 24 hours. Cell counting kit-8 (CCK-8) assay was performed to assess cell viability. b) to c) Human chondrocytes (HCs) of P3 (n = 3 in each group) were treated with different concentrations of 666-15 for two hours prior to b) IL-1 β (10 ng/ml) or c) CCCP (50 μ M) treatment for 24 hours. Cell viability was assessed using the CCK-8 assay. One-way analysis of variance was used to compare means among groups, and the Fisher's least significance difference test was used for multiple comparisons. *p < 0.05, ***p < 0.001.

medial tibial subchondral bone was defined as the region of interest. Images were binarized using the following grey-level thresholds in Hounsfield units: 80 to 255. The binarized images were then used to calculate morphological parameters using CTAn version 1.14.4 (Bruker Corporation), including bone mineral density (BMD, g/cm³), bone volume fraction (BV/TV, %), trabecular number (Tb.N, 1/mm), structure model index (SMI), trabecular bone pattern factor (Tb.Pf, 1/mm), and trabecular separation (Tb.Sp, mm).

Histological analysis and IHC assessment

Femoral head explants and left knee joint specimens without muscles were fixed in 4% paraformaldehyde at 4°C for 48 hours, and decalcified with 30% formic acid at room temperature for 24 to 72 hours. After being decalcified, the left joint tissues of guinea pigs, cut at half of the medial tibia plateau, were embedded in paraffin in the sagittal plane. For mice, the left joint tissues were embedded using paraffin in the coronal plane. After being roughly cut for to approximately 0.5 to 1 mm until the tissues were completely exposed, 25 to 35 sections, each with a thickness of 5 μ m, were prepared for histological examination and IHC assessment. Every fifth section was used for the safranin O and fast green (S/F) staining using the S/F solution (Applygen Technologies). The histological characteristics of cartilage were determined by two blinded observers using the Osteoarthritis Research Society International (OARSI) modified Mankin's score system for guinea pigs²⁷ and mice,²⁸ respectively. For IHC assessment, the sections were incubated with antibodies against p-CREB1 (Cell Signaling Technology; cat no. 9198; 1:500 dilution), aggrecan (Abcam; cat no. ab216965; 1:100 dilution), ADAMTS4 (Abcam; cat no. ab219548; 1:100 dilution), collagen II (Proteintech; cat no. 28459 to 1-AP; 1:50 dilution), and MMP13 (Proteintech; cat no. 18165 to 1-AP; 1:100 dilution) at 4°C overnight and followed by incubation with secondary antibody (Applygen; cat no. C1309; 1:1,000 dilution) for two hours at room temperature. The number of positively stained chondrocytes on the articular surface of each femoral head

or medial tibia plateau was counted and the percentage of positive cells was calculated.

ELISA

Cartilage oligomeric matrix protein (COMP) and C-terminal telopeptide of type II collagen (CTX-II) in serum were detected using the ELISA kit (Cloud-Clone, China) according to the manufacturer's instruction.

Immunoblotting

Immunoblotting analysis was performed as previously described.¹ In brief, cells were rinsed with cold phosphate-buffered saline (PBS), lysed on ice in lysis buffer, and boiled for ten minutes. Total cell lysates (about 30 μ g per lane) were then subjected to immunoblotting using primary antibodies against p-CREB1 (Cell Signaling Technology; cat no. 9198; 1:1,000 dilution) and ADAMTS4 (Abcam; cat no. ab185722; 1:1,000 dilution) at 4°C overnight, followed by incubation with secondary antibodies (Cell Signaling Technology, cat no. 7076, anti-mouse, HRP-linked antibody, 1:2,000 dilution; Cell Signaling Technology, cat no. 7074, anti-rabbit, HRP-linked antibody, 1:2,000 dilution) for two hours at room temperature. β -actin (Abcam; cat no. ab8226; 1:1,000) was used as the internal control.

Cell counting kit-8 assay

Cell viability was determined using the cell counting kit-8 (CCK-8) assay (Dojindo Molecular Technologies, Japan) according to the manufacturer's instruction. After incubation of human or guinea pig chondrocytes with or without drugs for indicated time, CCK-8 reagent was added to each well and then determined at a wavelength of 450 nm.

Determination of mitochondrial membrane potential by JC-10 dye staining

Mitochondrial membrane potential in human chondrocytes was determined by Mitochondrial Membrane Potential Kit (JC-10 assay; Solarbio, China) according to the instruction

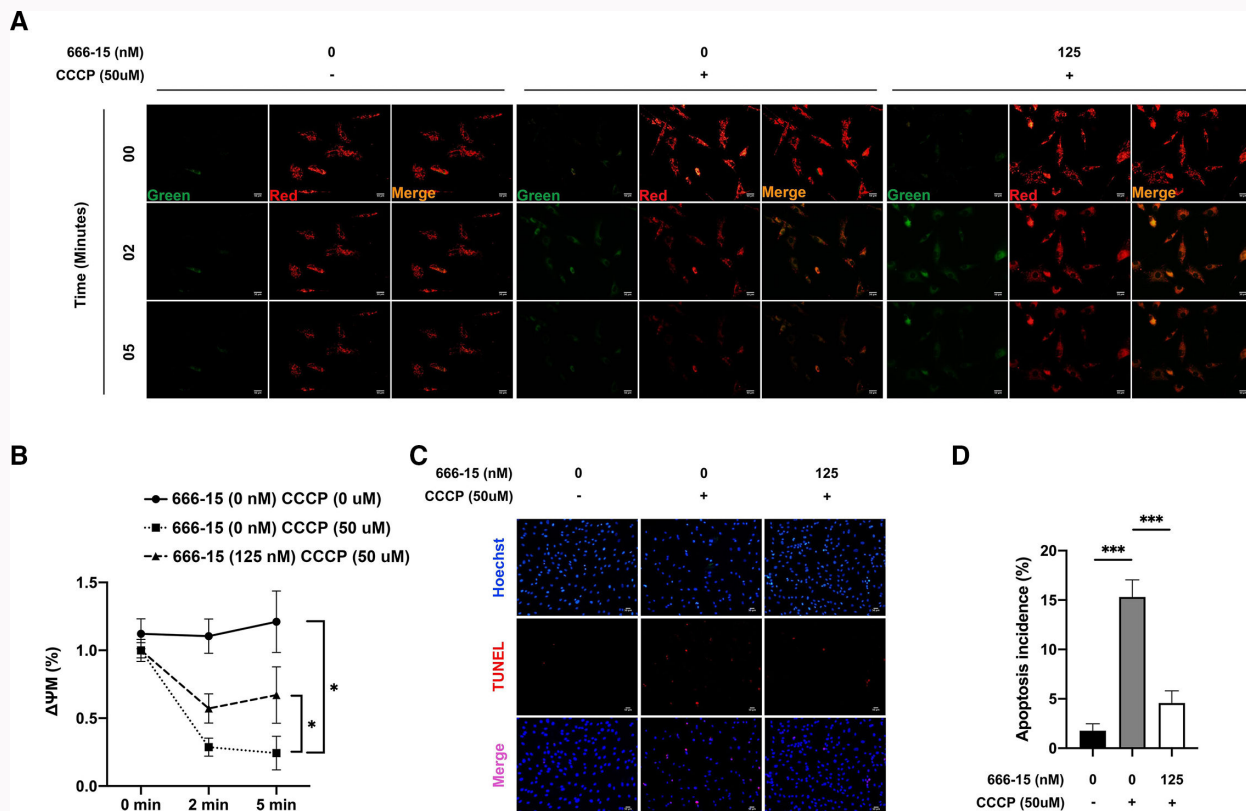


Fig. 5 HCs (n = 3 in each group) were pretreated with 666-15 (125 nM) for two hours and then stained with JC-10 dye followed by carbonyl cyanide 3-chlorophenylhydrazone (CCCP) (50 μ M) treatment at the indicated time. a) The JC-10 fluorescence was determined by a fluorescence microscope, and representative images are shown (scale bars = 50 μ m). b) Ratio of red/green JC-10 fluorescence was calculated to determine the mitochondrial membrane potential loss. c) and d) Measurement of apoptosis by terminal deoxynucleotidyl transferase dUTP nick end labelling (TUNEL) staining of human chondrocytes (HCs) (n = 3 in each group) pretreated with 666-15 (125 nM) for two hours and subsequently stained with JC-10 dye followed by CCCP (50 μ M) treatment for 24 hours. Cells were fixed and stained with TUNEL (red) and counterstained with Hoechst 33258 (blue) for visualization of nuclei. c) Representative images are shown (scale bars = 50 μ m). d) Quantification of TUNEL-positive nuclei. One-way analysis of variance was used to compare means among groups, and the Fisher's least significance difference test was used for multiple comparisons. *p < 0.05, ***p < 0.001.

of the manufacturer. Briefly, human chondrocytes pretreated with or without 666-15 (125 nM) for two hours were stained with JC-10 staining solution at 37°C for 20 minutes followed by CCCP (50 μ M) treatment for indicated time. Images were captured at indicated time using an Olympus IX-71 microscope (Japan).

Terminal deoxynucleotidyl transferase-mediated dUTP nick end-labelling

Human chondrocytes pretreated with or without 666-15 (125 nM) for two hours were incubated with CCCP (50 μ M) for 24 hours followed by TUNEL staining using a TUNEL detection kit (Applygen Technologies) according to the manufacturer's instruction. Nuclei were counterstained with Hoechst 33,258. Fluorescence staining was examined using an Olympus IX-71 microscope.

Statistical analysis

All data were presented as mean and standard deviation (SD). One-way analysis of variance (ANOVA) was used to compare means among groups. Additionally, the Fisher's least significant difference (LSD) multiple comparisons test was performed for the multiple comparisons. Prior to ANOVA, data were checked for normality using the Shapiro-Wilk test and for homogeneity of variance by Bartlett's test. Compari-

sons between two groups were analyzed using the independent-samples *t*-test. A p-value < 0.05 was considered to be statistically significant. The statistical analysis was performed using GraphPad Prism version 8.0 (GraphPad, USA).

Results

CREB1 is activated in osteoarthritic articular cartilage in vivo

To determine the exact role of CREB1 in OA, we first evaluated CREB1 activity in two different in vivo osteoarthritic animal models of OA: a spontaneous guinea pig model (Figure 1a to 1e) and an ACLT mouse model (Figure 1f to 1h). During early and progressive stages of spontaneous OA (from one to five months), a continual decrease in proteoglycan content was observed in the superficial and interterritorial region of the cartilage (Figure 1a). Obvious erosions were observed in the superficial zone of the cartilage at five months of age (Figure 1a). The OARSI score continually increased with age during the study period (Figure 1b). At the early stage of spontaneous OA (three months old), p-CREB1 expression was found in all zones, though predominantly in the superficial and middle zones of the cartilage (Figure 1c). During OA progression, we found a continual increase in the percentage of p-CREB1-positive chondrocytes in the articular cartilage from three to five months (Figure 1c to 1d). We also showed that CREB1 phosphorylation detected by immunoblotting

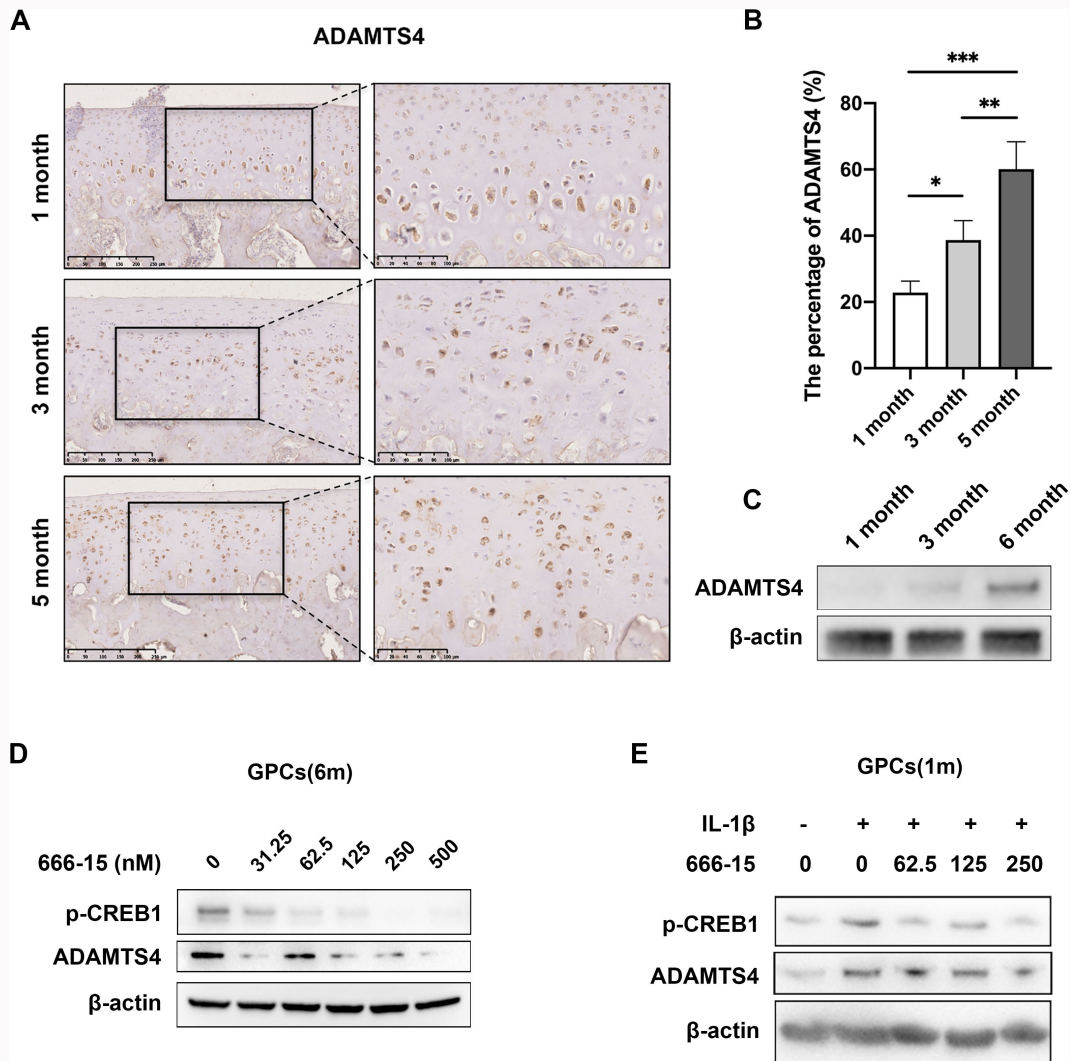


Fig. 6

666-15 was an inhibitor of a disintegrin and metalloproteinase with thrombospondin motifs 4 (ADAMTS4) with anti-catabolic activity in vitro. a) ADAMTS4 expression in the articular cartilage increased gradually with age. Representative images of immunohistochemical (IHC) staining of ADAMTS4 (left panel, scale bars = 250 μ m; right panel, scale bars = 100 μ m) in the articular cartilage of guinea pigs of different ages. b) Quantification of the ADAMTS4 IHC staining (n = 3 in each group). One-way analysis of variance was used to compare means among groups, and the Fisher's least significant difference test was used for multiple comparisons. *p < 0.05, **p < 0.01, ***p < 0.001. c) ADAMTS4 expressions in primary chondrocytes derived from guinea pigs (GPCs) of different ages were determined by immunoblotting. d) 666-15 inhibited ADAMTS4 expression in a dose-dependent manner. e) Interleukin-1 β (IL-1 β) induced upregulation of ADAMTS4 was suppressed by 666-15. p-CREB1, cAMP response element binding protein.

continually increased in chondrocytes with age (Figure 1e), which is consistent with the IHC staining of p-CREB1 in cartilage.

As expected, a similar phenomenon occurs in an OA mouse model. As can be seen from Figure 1f, sham-operated mice did not exhibit degenerative changes in articular cartilage, whereas six-week post-ACLT mice revealed heterogeneously distributed matrix with a severe loss of proteoglycan content in the superficial and middle zones of the tibial cartilage. Histological observations were quantitatively confirmed by the OARSI score as presented in Figure 1g. Furthermore, our IHC staining showed a significant increase in the percentage of p-CREB1-positive chondrocytes in the superficial and middle zones of the cartilage in ACLT mice, compared to that in sham-operated mice (Figure 1h). Our finding of drastically elevated cartilage CREB1 activity in both animal models indicates that increased cartilage CREB1

activity is a general feature during early and middle phases of OA.

CREB1 is activated in osteoarthritic cartilage explants ex vivo and chondrocytes in vitro

Interleukin-1 β (IL-1 β) is a key proinflammatory cytokine that promotes cartilage degradation and is involved in the pathogenesis of OA. Hence, IL-1 β is usually used as a mediator of OA progression.^{29,30} To investigate CREB1 activity in an IL-1 β -induced OA model, mouse femoral head explants were prepared and treated with IL-1 β for 72 hours, followed by the evaluation of p-CREB1 expression by IHC staining. As shown in Figure 2a, a severe loss of matrix was observed in the superficial zone of cartilage in IL-1 β -treated cartilage explants. Moreover, p-CREB1 expression was significantly upregulated in IL-1 β -treated cartilage explants, as evidenced by a significant increase in the percentage of p-CREB1-positive chondrocytes

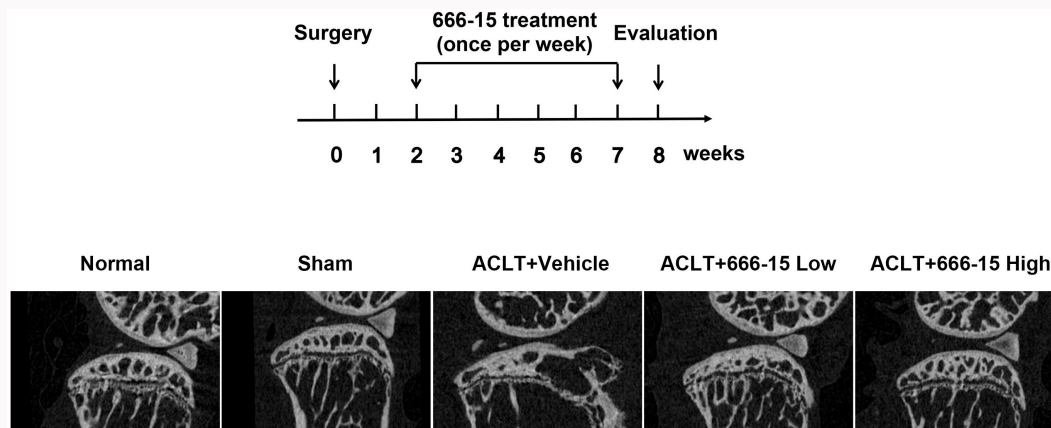


Fig. 7

666-15 improved deteriorated subchondral bone in an osteoarthritis mouse model with anterior cruciate ligament transection (ACLT). a) Schematic of the in vivo study design employed to investigate the effects of 666-15 on joint degeneration in ACLT mice. b) Representative μ CT images of the medial part of subchondral bone.

in the degenerative cartilage (Figures 2a to 2b). We next evaluated activation of CREB1 in IL-1 β -induced OA-like primary chondrocytes. We found that human primary chondrocytes treated with IL-1 β exhibited activation of CREB1 in a timely and pulsatile manner (Figure 2c).

CCCP is a widely used inducer of mitochondrial dysfunction. It has been recently reported that mitochondrial dysfunction induced by CCCP treatment was associated with increased apoptosis and enhanced expression of catabolic genes in chondrocytes in OA.³¹ Thus, CCCP can also be used as a potential mediator of OA progression. Here, we assessed CREB1 activity in CCCP-treated human primary chondrocytes. As shown in Figure 2d, CREB1 was activated by CCCP in a manner similar to that by IL-1 β . Taken together, these results indicate that CREB1 activation could be involved in IL-1 β - or CCCP-mediated OA pathogenesis.

Inhibition of CREB1 by 666-15 enhances cell viability of OA-like chondrocytes in vitro

We next investigated the effect of CREB1 inhibition by 666-15 (Figure 3a) on viability of OA-like chondrocytes. We first performed a comparison of collagen II expression as well as cell viability among chondrocytes obtained from the knees of guinea pigs of different ages. Our results showed that chondrocytes became less active and gradually lost their cartilage phenotype with age, as evidenced by the declined cell viability and collagen II expression with age (Figure 3b and Supplementary Figure a). Moreover, in comparison to the control group (666-15 concentration was 0 nM), concentrations of 666-15 from 62.5 to 500 nM drastically decreased protein level of p-CREB1 and significantly improved cell viability of aged guinea pig chondrocytes (Figure 3c to 3d). It has been reported that articular chondrocytes tend to lose their cartilage phenotype after successive subcultures on regular plastic dishes.^{32,33} As expected, treatment of successively passaged human chondrocytes with various concentrations of 666-15 also inhibited CREB1 activity and significantly enhanced cell viability (Figure 3e to 3f). Taken together, these results suggested that hyperactivated CREB1 might be responsible for the decreased cell viability of OA-like chondrocytes.

666-15 alleviates IL-1 β - or CCCP-induced chondrocyte injury through inhibition of mitochondrial dysfunction-associated apoptosis

We further investigated the effect of 666-15 on IL-1 β - or CCCP-induced chondrocyte injury. As can be seen from Figure 4, 666-15 in various concentrations significantly alleviated IL-1 β - or CCCP-induced chondrocyte injury ($p < 0.05$). Since both IL-1 β and CCCP can induce mitochondrial dysfunction that accounts for increased apoptosis in chondrocytes,³¹ we next determined the effect of 666-15 on mitochondrial dysfunction-associated apoptosis induced by CCCP. Indeed, we found a significant loss of mitochondrial membrane potential in chondrocytes upon CCCP stimulation, as evidenced by a rapid decrease in the red fluorescence and increase in green fluorescence of JC-10 dye within five minutes of CCCP (50 μ M) treatment (Figure 5). However, pretreatment with 666-15 considerably inhibited CCCP-induced mitochondrial dysfunction. Moreover, the application of 666-15 prior to CCCP stimulation significantly suppressed CCCP-induced apoptosis. These results indicated that 666-15 suppressed mitochondrial dysfunction-associated apoptosis, thereby alleviating IL-1 β - or CCCP-induced chondrocyte injury.

Inhibition of CREB1 by 666-15 suppresses ADAMTS4 expression

Since MMP13 and ADAMTS4 are two of the most critical matrix-degrading enzymes in OA, and CREB1 has been suggested to induce MMP13 in osteoarthritic cartilage,¹⁸ we hypothesized that ADAMTS4 might also be regulated by CREB1 in OA. Similar to the expression pattern of CREB1, there is a continual increase in the IHC staining of ADAMTS4 in the articular cartilage with age (Figure 6ab). Consistently, expression of ADAMTS4 measured by immunoblotting continually increased in chondrocytes with age (Figure 6c). To investigate the role of inhibition of CREB1 on ADAMTS4 expression, we inhibited CREB1 activity by 666-15. As shown in Figure 6d and Supplementary Figure b, a decrease in ADAMTS4 protein levels was observed in aged guinea pig chondrocytes cultured in the presence of 666-15 in various concentrations compared to the control group. Moreover, pretreatment of chondrocytes with 666-15 significantly

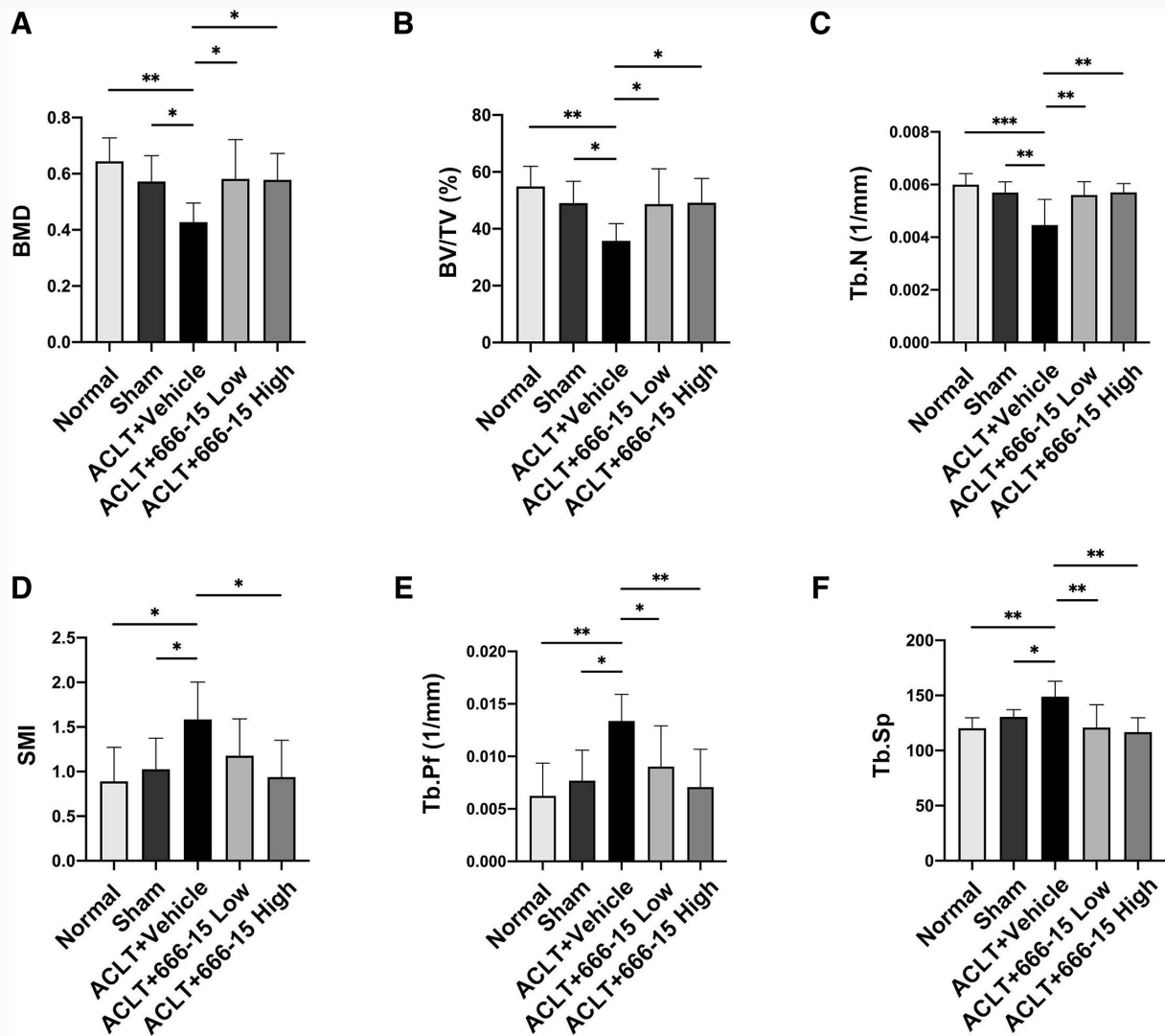


Fig. 8

a) to f) Quantitative μ CT analysis of subchondral bone. (n = 5 in each group). One-way analysis of variance was used to compare means among groups and the Fisher's least significant difference test was used for multiple comparisons. *p < 0.05, **p < 0.01, ***p < 0.001. ACLT, anterior cruciate ligament transection; BMD, bone mineral density; BV/TV, bone volume fraction; SMI, structure model index; Tb.N, trabecular number; Tb.Pf, trabecular bone pattern factor; Tb.Sp, trabecular separation.

suppressed IL-1 β -induced ADAMTS4 protein increase (Figure 6e and Supplementary Figure b). Taken together, ADAMTS4 expression can be suppressed through inhibition of CREB1 by 666-15.

666-15 alleviates OA in an ACLT mouse model

Next, we evaluated whether 666-15 could maintain the microstructure of subchondral bone and cartilage in an ACLT mouse model. A schematic of the in vivo study design employed to investigate the effects of 666-15 on joint degeneration in ACLT mice is depicted in Figure 7a. The micro-CT findings showed severe bone loss in ACLT mice (Figure 7b), as verified by reductions in BMD, BV/TV, and Tb.N, and increases in SMI, Tb.Pf, and Tb.Sp in subchondral trabecular bone, compared with either the normal group or the sham group (Figure 8). 666-15 administration significantly improved bone microstructure evidenced by dose-independently reversing the decreases in BMD, BV/TV, and Tb.N, as well as the increases in SMI, Tb.Pf, and Tb.Sp in mice with

ACLT. S/F staining revealed a severe loss of cartilage matrix in mice with ACLT compared to either the normal group or the sham group (Figure 9a). The OARSI score of the vehicle group was significantly higher than that of either the normal group or the sham group (Figure 9b). 666-15 administrations significantly prevented cartilage degeneration as depicted in Figures 9 and 10. In addition, the effects of 666-15 on CREB1 activity as well as expression of anabolic (aggrecan and collagen II) proteins and catabolic (ADAMTS4 and MMP13) enzymes in cartilage tissues were examined by IHC staining (Figure 10). Inhibition of CREB1 by 666-15 significantly enhanced the expression of anabolic proteins while suppressing the expression of catabolic enzymes, indicating that 666-15 was able to diminish cartilage degeneration in ACLT mice. Furthermore, analysis of serum markers of cartilage turnover, which serve as predictors of cartilage loss, confirmed that 666-15 at doses of 5 mg/kg and 10 mg/kg considerably decreased the cartilage collagen degradation-related markers cartilage oligomeric matrix protein (COMP) and type II

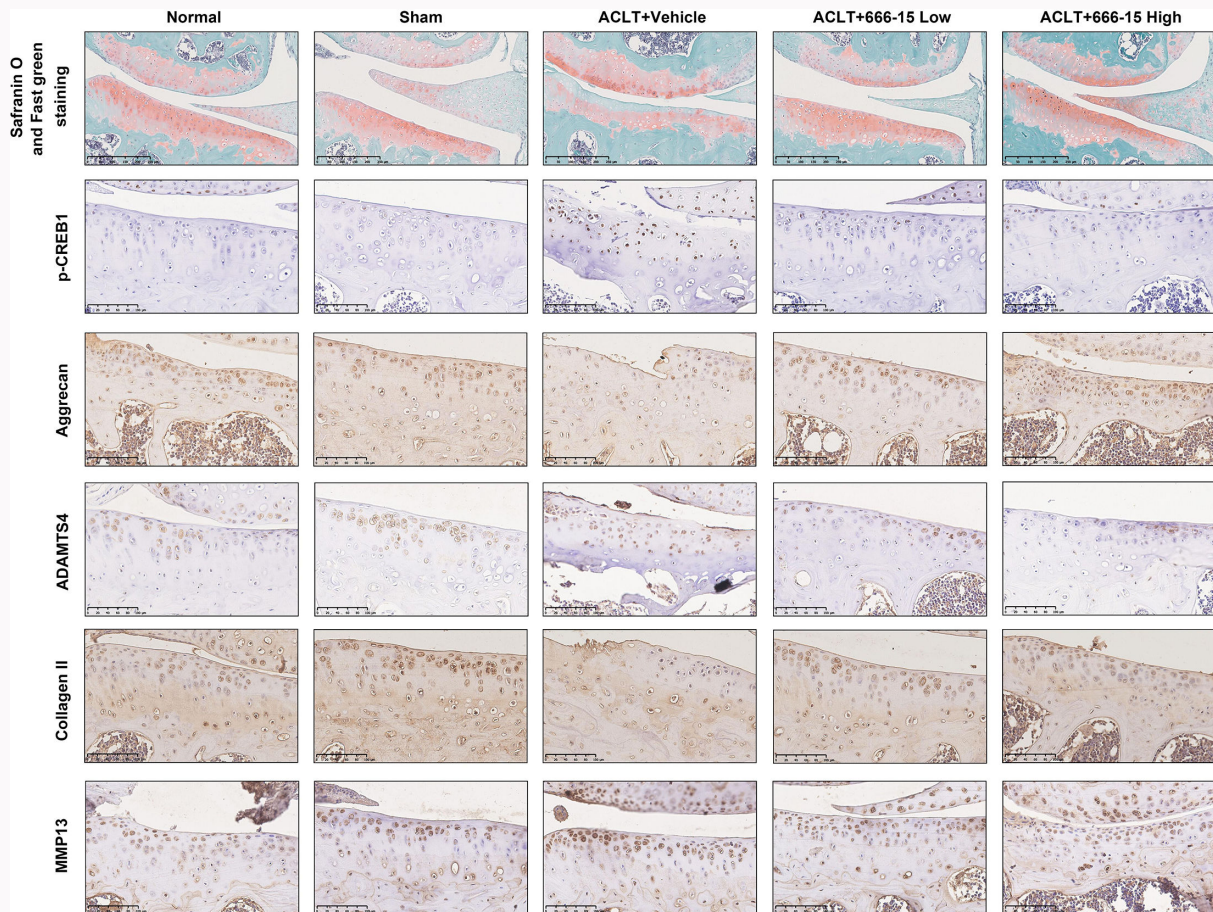


Fig. 9

666-15 alleviated anterior cruciate ligament transection (ACLT)-induced articular cartilage degeneration. Representative micrographs of S/F staining of the cartilage of each group (scale bars = 250 μ m) and IHC staining of cAMP response element binding protein (p-CREB1), aggrecan, a disintegrin and metalloproteinase with thrombospondin motifs 4 (ADAMTS4), collagen II, and matrix metalloproteinase 13 (MMP13) in the cartilage of each group (scale bars = 100 μ m).

collagen telopeptides (CTX-II) compared to the vehicle group. Moreover, we have also conducted a study on the effect of 666-15 on synovitis in ACLT-induced OA mice. We found that ACLT resulted in the synovial hyperplasia, while 666-15 administration was able to alleviate ACLT-induced lesions in synovial membrane as evidenced by decreased synovitis score (Supplementary Figure c), suggesting a protective effect of 666-15 on synovial membrane.

To assess the safety of intraperitoneally supplementing high doses of 666-15, the mice had their weight monitored for the duration of the study. The initial and final body weights did not vary among the different experimental groups (Supplementary Figure d), suggesting no adverse effects of 666-15, which is consistent with the findings of a previous study.²³

Discussion

The major objectives of OA management are to achieve symptomatic relief, functional recovery, and/or joint structure modification. Despite the high prevalence of OA, therapeutic options remain limited. The standard pharmacological therapy for OA mainly involves analgesics and non-steroidal anti-inflammatory drugs. However, there is still a lack of regulatory agency-approved disease-modifying drugs for OA that may arrest disease progression by ameliorating symptoms (pain

relief and/or physical function improvement) and delaying joint structure change.

The present study is the first to evaluate the effect of the CREB1 inhibitor 666-15 in OA. We demonstrated that CREB1 is hyperactive in osteoarthritic articular cartilage and chondrocytes. Inhibition of CREB1 by 666-15 enhances viability of OA-like chondrocytes and alleviates IL-1 β - or CCCP-induced chondrocyte injury through inhibition of mitochondrial dysfunction-associated apoptosis. Moreover, 666-15 administration alleviates the joint degeneration in an ACLT mouse model.

CREB1 is frequently dysregulated in various pathologies.¹⁴⁻¹⁶ Previous studies demonstrated that CREB1 activity is positively associated with hip OA.¹⁹ Moreover, CREB1 was identified to be potentially one of the critical transcriptional factors that are involved in the regulation of OA.¹⁷ However, it has also been reported that downregulation of CREB1 inhibits cell proliferation and aggravates inflammation.²⁰ Together, these data support the idea that abnormal activation of CREB1 is involved in OA by functioning as either a promoter or a suppressor. In this study, we confirmed that CREB1 is hyperactivated in osteoarthritic articular cartilage *in vivo*, cartilage explant *ex vivo*, and chondrocytes *in vitro*, suggesting its potential promoter-like role in OA, as evidenced by CCK-8 assay, JC-10 staining assay, and TUNEL staining assay.

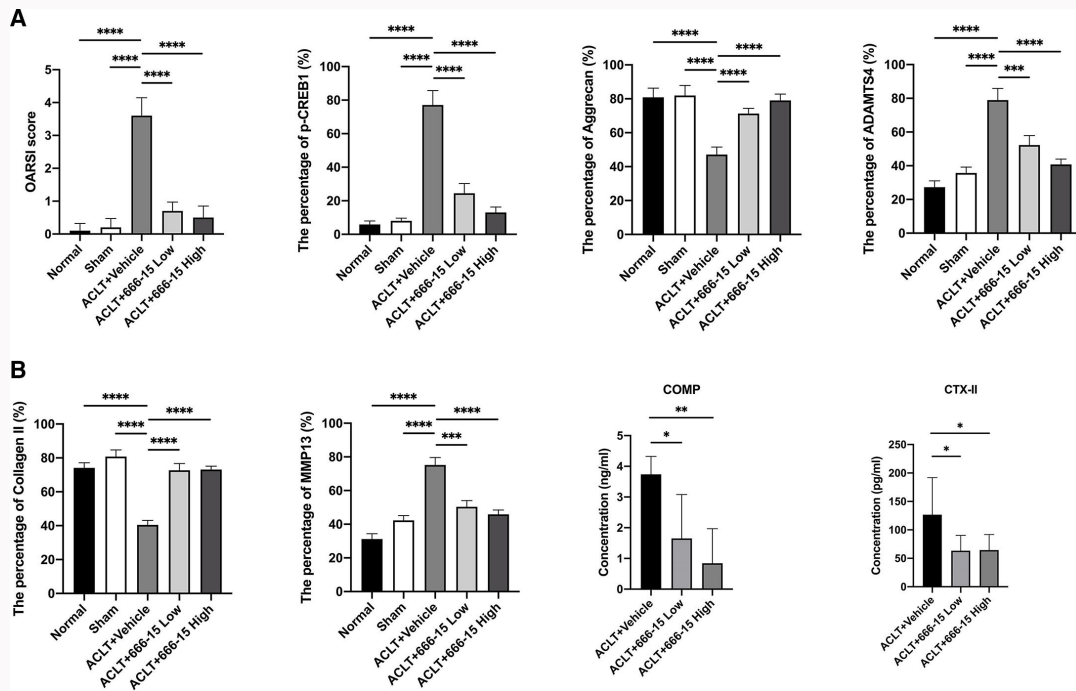


Fig. 10

a) Osteoarthritis Research Society International (OARS1) score of coronal sections of the medial tibia plateau of the mice described in Figure 9 (n = 5 in each group). Quantifications of IHC staining of: b) p-CREB1; c) aggrecan; d) ADAMTS4; e) collagen II; and f) MMP13 (n = 5 in each group). Serum levels of g) cartilage oligomeric matrix protein (COMP) and h) C-terminal telopeptide of type II collagen (CTX-II) in each group were measured using enzyme-linked immunosorbent assay (ELISA) (n = 5 in each group). Analysis of variance was used to compare means among groups and the Fisher's least significant difference test was used for multiple comparisons. *p < 0.05, **p < 0.01, ***p < 0.001, ****p < 0.0001.

OA is characterized by progressive destruction of articular cartilage that is primarily due to the loss of chondrocytes, which are the single cell population in cartilage and are responsible for maintaining a homeostatic equilibrium between production and degradation of cartilage ECM. Under the stimulation of inflammatory cytokines, the remaining chondrocytes exhibit an abnormal catabolic phenotype that leads to an imbalance between degradation and synthesis of ECM. Besides the well-characterized matrix metalloproteinases (MMPs), ADAMTSs are the principal proteases expressed in cartilage. ADAMTS4 in particular is the main protease that displays significantly altered expression in OA and is thus a potential therapeutic target for OA treatment. It has been reported that CREB1 regulates MMP13 expression in osteoarthritic cartilage.¹⁸ However, its impact on cartilage catabolism driven by other ADAMTSs is not fully understood. In the present study, we found that ADAMTS4 is upregulated in osteoarthritic articular cartilage in vivo, and is positively regulated by CREB1. We demonstrated that the CREB1/ADAMTS4 axis is activated in OA, and that agents targeting the CREB1/ADAMTS4 axis might be effective in maintaining ECM homeostasis to attenuate the progression of OA.

Chondrocyte viability is a vital feature crucial for the maintenance of cartilage structure and integrity. As a potent and specific CREB1 inhibitor, 666-15 inhibits CREB1 activation in several types of cells. It also exerts efficacious antitumour effects without overt toxicity in the MDA-MB-468 or synovial sarcoma cells xenograft model.^{23,24} Nevertheless, whether 666-15 protects against cartilage degeneration remains poorly understood. In our study, we demonstrated that 666-15 administrations considerably counteract in vitro IL-1 β - or

CCCP-dependent chondrocyte injury and catabolic events. Moreover, we also showed that 666-15 exhibits a chondroprotective effect, evidenced by reduced OARS1 scores concomitant with a reduction in catabolic enzyme expressions, and an increase in anabolic protein contents in a murine post-traumatic OA model.

CREB1 plays a core role in mediating cellular responses to stress.^{34,35} It has been reported that CREB1 can elevate an oxidative stress-induced senescence in granulosa cells by reducing the mitochondrial function.³⁴ Mechanistically, it was shown that the biogenesis of ageing granulosa cells is subject to CREB1 binding to the upstream promoters of protein kinase AMP-activated catalytic subunit alpha 1 (PRKAA1) and 2 (PRKAA2), the key effectors of mitochondrial biogenesis.³⁴ A recent study demonstrated that CREB1 is an important transcription factor that promotes oxidative stress-induced apoptosis by suppressing expression of B-crystallin, a strong anti-apoptotic regulator, in both rat lens organ culture and mouse lens epithelial cells.³⁵ In the present study, we observed that CREB1 plays an important role in CCCP- or IL-1 β -induced stress response in chondrocytes. Both CCCP and IL-1 β have been identified as inducers of mitochondrial dysfunction in chondrocytes, as evidenced by loss of mitochondrial membrane potential and apoptosis.³¹ We found that treatment of chondrocytes with CCCP or IL-1 β could stimulate activation of CREB1 in a timely and pulsative manner. Moreover, inhibition of CREB1 by 666-15 was able to alleviate CCCP- or IL-1 β -induced chondrocyte injury and inhibit apoptosis associated with mitochondrial dysfunction. Since CREB1 plays the key role of mitochondria biogenesis and apoptosis,^{34,35} we strongly believe that inhibition of CREB1 activation may protect against

CCCP- or IL-1 β -induced chondrocyte death by regulating the expression of genes involved in mitochondrial biogenesis and apoptosis, which requires further investigation.

Accumulating evidence reveals that OA is a multifactorial joint disease,^{36,37} affecting not only the articular cartilage but also the subchondral bone. It has been well established that abnormal mechanical loading during ACLT-induced OA onset results in overactivated osteoclastogenesis and bone resorption in the subchondral bone.³⁸ Consistent with multiple previous studies,³⁹⁻⁴¹ ACLT mice in our study also exhibited subchondral bone loss. Previous studies have reported that CREB1 is a crucial mediator of signal-dependent transcription that regulates differentiation processes in osteoclastogenesis, and activation of CREB1 signalling promotes osteoclastogenesis.^{42,43} Other research groups have also reported that ACLT-induced subchondral bone loss has been proved to be primarily achieved by osteoclastogenesis induced by receptor activator of nuclear factor-kappa B ligand (RANKL), a direct target of CREB1.^{44,45} Based on the above literature review, we suggest that inhibition of CREB1 activity may potentially impede ACLT-induced overactivated osteoclastogenesis. Besides the anti-cartilage degeneration effect, we have also demonstrated in our study that CREB1 inhibitor 666-15 helped maintain the microstructure of subchondral bone, as evidenced by a rescue in BMD, BV/TV, Tb.N, SMI, Tb.Pf, and Tb.Sp in subchondral trabecular bone after ACLT surgery when compared with either the normal group or the sham group. Previous studies have shown that mitochondrial dysfunction impairs osteogenesis and is associated with accelerated bone loss during the ageing process.⁴⁶ However, it is not clear whether mitochondrial dysfunction is involved in ACLT-induced subchondral bone loss. Due to the multifaceted crosstalk among the bone remodelling associated cells (including osteoclasts, osteoblasts, and osteocytes), however, the exact mechanism underlying the inhibitory effect of 666-15 on aberrant joint subchondral bone remodelling has yet to be explored further. Moreover, additional studies are needed to fully understand the role of CREB1 activation and mitochondrial dysfunction in the subchondral bone compartment, and their contribution to the development of OA.

It is frequently acknowledged that OA is a heterogeneous disease that exhibits multiple phenotypes, such as post-traumatic, pain, ageing, metabolic, and genetic.⁴⁷ In our study, we highlighted the therapeutic potential of 666-15 in diminishing OA deterioration in a mouse post-traumatic OA model where we used the ACLT method to induce joint instability and pathological changes. Given these complicated phenotypes of OA, the anti-OA effect of 666-15 needs to be further investigated in additional OA animal models of different OA phenotypes.

In summary, our work demonstrated that hyperactive CREB1 plays a critical role in the development of OA. Furthermore, our study is the first to apply CREB1 inhibitor 666-15 to the treatment of OA. We demonstrated that 666-15 exerts *in vitro* anti-IL-1 β or -CCCP effects in chondrocytes, and drastically diminishes the severity of post-traumatic OA in mice. Together these findings unveiled 666-15 as a very promising anti-OA drug.

There are several limitations to our study. First, we did not evaluate whether CREB1 inhibitor 666-15 could reduce osteoarthritic knee pain, the dominant clinical symptom,

in our animal study. Second, it is unfortunate that we were unable to define the therapeutic effect of 666-15 in OA patients. Third, ADAMT5, another important enzyme responsible for aggrecan loss, was not detected in the present study. Fourth, the sample size of animals used in our study is based on the literature, and we acknowledge that this may have its limitations. Fifth, 666-15 was intraperitoneally supplemented in our study, however we were unfortunately unable to detect the quantity of 666-15 in the synovial fluid of the knee joint in our study. The amount of drug that reaches the specific organs after intraperitoneal injection mainly depends on liver metabolism, tissue retention and distribution, and excretion. Instead, we used IHC analysis to detect CREB1 activity, an indicator of the effectiveness of 666-15. Additionally, an intraperitoneal injection might have systemic effects. To rule out the possible side-effects, we assessed the safety of intraperitoneally supplementing high doses of 666-15 through monitoring the changes of the weights of the mice during the study duration. Based on the body weights monitored, it showed that there are no adverse effects of 666-15, which is consistent with the findings of a previous study.²³ Moreover, we recommend that caution should obviously be exercised in extrapolating these findings from *in vitro* experiments and animal studies to clinical settings. As our understanding of the various signalling pathways involved in the pathogenesis of OA has quickly and greatly evolved in recent years, a surge of candidate targets and pathways for the development of new therapeutic strategies has emerged. The question then arises as to how to determine the most effective candidate for the treatment of OA. We believe that the choice of candidate for OA drug development should be based on the evidence that it is involved in the regulation of a broad range of important pathophysiological processes of this disease. These processes include imbalanced cartilage remodelling through dysregulated anabolic and catabolic processes, as well as aberrant subchondral bone remodelling via regulation of bone cells, including osteoclasts, osteoblasts, and osteocytes. Drug development for OA needs to meet both clinical symptom relief and joint structure improvement. However, as OA is a heterogeneous condition with complex and variable clinical phenotypes and molecular endotypes in varying degrees at different stages of this disease, using a single therapeutic agent targeting a sole target or pathway might be unlikely to succeed in managing OA in a clinical setting. Therefore, the strategy of employing a combination of drugs targeting different processes of OA should be considered as analogous to the approach used in cancer treatment.⁴⁸ The selection or combination of the factor(s) that would provide the best protection against OA also remains to be demonstrated.

Supplementary material

Figures showing collagen II expression among chondrocytes obtained from the knees of guinea pigs of different ages, densitometry analysis of the immunoblotting data of p-cAMP response element binding protein regulation of a disintegrin and metalloproteinase with thrombospondin motifs 4 expression, the effect of 666-15 on synovitis in anterior cruciate ligament transection-induced osteoarthritic mice, as well as the monitoring of body weights after the administration of 666-15.

References

1. Wang Y, Wu C, Tao J, Zhao D, Jiang X, Tian W. Differential proteomic analysis of tibial subchondral bone from male and female guinea pigs with spontaneous osteoarthritis. *Exp Ther Med*. 2021;21(6):633.
2. Ripmeester EGJ, Timur UT, Caron MMJ, Welting TJM. Recent insights into the contribution of the changing hypertrophic chondrocyte phenotype in the development and progression of osteoarthritis. *Front Bioeng Biotechnol*. 2018;6:18.
3. Glyn-Jones S, Palmer AJR, Agricola R, et al. Osteoarthritis. *Lancet*. 2015;386(9991):376–387.
4. Buckwalter JA, Mankin HJ. Articular cartilage: tissue design and chondrocyte-matrix interactions. *Instr Course Lect*. 1998;47:477–486.
5. Griffith LA, Arnold KM, Sengers BG, Tare RS, Houghton FD. A scaffold-free approach to cartilage tissue generation using human embryonic stem cells. *Sci Rep*. 2021;11(1):18921.
6. Sophia Fox AJ, Bedi A, Rodeo SA. The basic science of articular cartilage: structure, composition, and function. *Sports Health*. 2009;1(6):461–468.
7. Smith GN. The role of collagenolytic matrix metalloproteinases in the loss of articular cartilage in osteoarthritis. *Front Biosci*. 2006;11:3081–3095.
8. Swingle TE, Waters JG, Davidson RK, et al. Degradome expression profiling in human articular cartilage. *Arthritis Res Ther*. 2009;11(3):R96.
9. Wang M, Sampson ER, Jin H, et al. MMP13 is a critical target gene during the progression of osteoarthritis. *Arthritis Res Ther*. 2013;15(1):R5.
10. Naito S, Shiomi T, Okada A, et al. Expression of ADAMTS4 (aggrecanase-1) in human osteoarthritic cartilage. *Pathol Int*. 2007;57(11):703–711.
11. Enochson L, Stenberg J, Brittberg M, Lindahl A. GDF5 reduces MMP13 expression in human chondrocytes via DKK1 mediated canonical Wnt signaling inhibition. *Osteoarthritis Cartilage*. 2014;22(4):566–577.
12. Wang Y, Hu Z, Liu Z, et al. MTOR inhibition attenuates DNA damage and apoptosis through autophagy-mediated suppression of CREB1. *Autophagy*. 2013;9(12):2069–2086.
13. Mayr B, Montminy M. Transcriptional regulation by the phosphorylation-dependent factor CREB. *Nat Rev Mol Cell Biol*. 2001;2(8):599–609.
14. Watson MJ, Berger PL, Banerjee K, et al. Aberrant CREB1 activation in prostate cancer disrupts normal prostate luminal cell differentiation. *Oncogene*. 2021;40(18):3260–3272.
15. Zhang Z, Guan B, Li Y, He Q, Li X, Zhou L. Increased phosphorylated CREB1 protein correlates with poor prognosis in clear cell renal cell carcinoma. *Transl Androl Urol*. 2021;10(8):3348–3357.
16. Ohayon S, Yitzhaky A, Hertzberg L. Gene expression meta-analysis reveals the up-regulation of CREB1 and CREBBP in Brodmann Area 10 of patients with schizophrenia. *Psychiatry Res*. 2020;292:113311.
17. Li G, Han N, Li Z, Lu Q. Identification of transcription regulatory relationships in rheumatoid arthritis and osteoarthritis. *Clin Rheumatol*. 2013;32(5):609–615.
18. Bui C, Barter MJ, Scott JL, et al. cAMP response element-binding (CREB) recruitment following a specific CpG demethylation leads to the elevated expression of the matrix metalloproteinase 13 in human articular chondrocytes and osteoarthritis. *FASEB J*. 2012;26(7):3000–3011.
19. Ji B, Ma Y, Wang H, Fang X, Shi P. Activation of the P38/CREB/MMP13 axis is associated with osteoarthritis. *Drug Des Devel Ther*. 2019;13:2195–2204.
20. Wang Z, Ni S, Zhang H, Fan Y, Xia L, Li N. Silencing SGK1 alleviates osteoarthritis through epigenetic regulation of CREB1 and ABCA1 expression. *Life Sci*. 2021;268:118733.
21. Yan J, Xu W, Lenahan C, et al. CCR5 activation promotes NLRP1-dependent neuronal pyroptosis via CCR5/PKA/CREB pathway after intracerebral hemorrhage. *Stroke*. 2021;52(12):4021–4032.
22. Guan X, Wang Y, Kai G, et al. Cerebrolysin ameliorates focal cerebral ischemia injury through neuroinflammatory inhibition via CREB/PGC-1 α pathway. *Front Pharmacol*. 2019;10:1245.
23. Xie F, Li BX, Kassenbrock A, et al. Identification of a potent inhibitor of CREB-mediated gene transcription with efficacious in vivo anticancer activity. *J Med Chem*. 2015;58(12):5075–5087.
24. Cyra M, Schulte M, Berthold R, et al. SS18-SSX drives CREB activation in synovial sarcoma. *Cell Oncol (Dordr)*. 2022;45(3):399–413.
25. Fu L, Hu Y, Song M, et al. Up-regulation of FOXD1 by YAP alleviates senescence and osteoarthritis. *PLoS Biol*. 2019;17(4):e3000201.
26. Deng L, Ren R, Liu Z, et al. Stabilizing heterochromatin by DGCR8 alleviates senescence and osteoarthritis. *Nat Commun*. 2019;10(1):3329.
27. Kraus VB, Huebner JL, DeGroot J, Bendele A. The OARSI histopathology initiative - recommendations for histological assessments of osteoarthritis in the guinea pig. *Osteoarthritis Cartilage*. 2010;18 Suppl 3(Suppl 3):S35–52.
28. Glasson SS, Chambers MG, Van Den Berg WB, Little CB. The OARSI histopathology initiative - recommendations for histological assessments of osteoarthritis in the mouse. *Osteoarthritis Cartilage*. 2010;18 Suppl 3:S17–23.
29. Luobu Z, Wang L, Jiang D, Liao T, Luobu C, Qunpei L. CircSCAPER contributes to IL-1 β -induced osteoarthritis in vitro via miR-140-3p/EZH2 axis. *Bone Joint Res*. 2022;11(2):61–72.
30. Wang M, Tan G, Jiang H, et al. Molecular crosstalk between articular cartilage, meniscus, synovium, and subchondral bone in osteoarthritis. *Bone Joint Res*. 2022;11(12):862–872.
31. Ansari MY, Ahmad N, Voleti S, Wase SJ, Novak K, Haqqi TM. Mitochondrial dysfunction triggers a catabolic response in chondrocytes via ROS-mediated activation of the JNK/AP1 pathway. *J Cell Sci*. 2020;133(22):jcs247353.
32. Wu G-X, Chen C-Y, Wu C-S, Hwang L-C, Yang S-W, Kuo S-M. Restoration of the phenotype of dedifferentiated rabbit chondrocytes by sesquiterpene farnesol. *Pharmaceutics*. 2022;14(1):186.
33. Han F, Zhu C, Guo Q, Yang H, Li B. Cellular modulation by the elasticity of biomaterials. *J Mater Chem B*. 2016;4(1):9–26.
34. Lin P-H, Lin L-T, Li C-J, et al. Combining bioinformatics and experiments to identify CREB1 as a key regulator in senescent granulosa cells. *Diagnostics (Basel)*. 2020;10(5):295.
35. Wang L, Nie Q, Gao M, et al. The transcription factor CREB acts as an important regulator mediating oxidative stress-induced apoptosis by suppressing α B-crystallin expression. *Aging (Albany NY)*. 2020;12(13):13594–13617.
36. Rainbow R, Ren W, Zeng L. Inflammation and joint tissue interactions in OA: Implications for potential therapeutic approaches. *Arthritis*. 2012;2012:741582.
37. Neogi T. Clinical significance of bone changes in osteoarthritis. *Ther Adv Musculoskelet Dis*. 2012;4(4):259–267.
38. Fang C, Guo J-W, Wang Y-J, et al. Di-tert-butyl phthalate attenuates osteoarthritis in ACLT mice via suppressing ERK/c-fos/NFATc1 pathway, and subsequently inhibiting subchondral osteoclast fusion. *Acta Pharmacol Sin*. 2022;43(5):1299–1310.
39. Zhou F, Mei J, Han X, et al. Kinsenoside attenuates osteoarthritis by repolarizing macrophages through inactivating NF- κ B/MAPK signaling and protecting chondrocytes. *Acta Pharm Sin B*. 2019;9(5):973–985.
40. Cui Z, Crane J, Xie H, et al. Halofuginone attenuates osteoarthritis by inhibition of TGF- β activity and H-type vessel formation in subchondral bone. *Ann Rheum Dis*. 2016;75(9):1714–1721.
41. Zou Z-L, Sun M-H, Yin W-F, Yang L, Kong L-Y. Avicularin suppresses cartilage extracellular matrix degradation and inflammation via TRAF6/MAPK activation. *Phytomedicine*. 2021;91:153657.
42. Liu C, Han Y, Zhao X, et al. POLR2A blocks osteoclastic bone resorption and protects against osteoporosis by interacting with CREB1. *J Cell Physiol*. 2021;236(7):5134–5146.
43. Park KH, Gu DR, Jin SH, et al. Pueraria iobate inhibits RANKL-mediated osteoclastogenesis via downregulation of CREB/PGC1 β /c-Fos/NFATc1 signaling. *Am J Chin Med*. 2017;45(8):1725–1744.
44. Ma L, Zhao X, Liu Y, Wu J, Yang X, Jin Q. Dihydroartemisinin attenuates osteoarthritis by inhibiting abnormal bone remodeling and angiogenesis in subchondral bone. *Int J Mol Med*. 2021;47(3):04855.
45. Wen X, Hu G, Xiao X, et al. FGF2 positively regulates osteoclastogenesis via activating the ERK-CREB pathway. *Arch Biochem Biophys*. 2022;727:109348.
46. Dobson PF, Dennis EP, Hipps D, et al. Mitochondrial dysfunction impairs osteogenesis, increases osteoclast activity, and accelerates age related bone loss. *Sci Rep*. 2020;10(1):11643.
47. Mével E, Merceron C, Vinatier C, et al. Olive and grape seed extract prevents post-traumatic osteoarthritis damages and exhibits in vitro anti IL-1 β activities before and after oral consumption. *Sci Rep*. 2016;6:33527.
48. Oo WM, Little C, Duong V, Hunter DJ. The development of disease-modifying therapies for osteoarthritis (DMOADs): The evidence to date. *Drug Des Devel Ther*. 2021;15:2921–2945.

Author information

Y. Wang, PhD, Associate Professor

Z. Wu, M.Med., Research Assistant

S. Li, PhD, Assistant Professor

Y. Zhang, BSc, Senior Technician

C. Wu, PhD, Professor

Department of Molecular Orthopedics, National Center for Orthopaedics, Beijing Research Institute of Traumatology and Orthopaedics, Beijing Jishuitan Hospital, Capital Medical University, Beijing, China.

G. Yan, M.Agr., Senior Technician, National Center for Orthopaedics, Animal Laboratory, Beijing Research Institute of Traumatology and Orthopaedics, Beijing Jishuitan Hospital, Capital Medical University, Beijing, China.

G. Li, BSc, Senior Technician, National Center for Orthopaedics, Laboratory of Bone Tissue Engineering, Beijing Research Institute of Traumatology and Orthopaedics, Beijing Jishuitan Hospital, Capital Medical University, Beijing, China.

Author contributions

Y. Wang: Conceptualization, Methodology, Investigation, Formal analysis, Writing – original draft, Writing – review & editing.

Z. Wu: Conceptualization, Methodology, Investigation, Formal analysis, Writing – original draft.

G. Yan: Investigation.

S. Li: Investigation.

Y. Zhang: Investigation.

G. Li: Investigation.

C. Wu: Conceptualization, Methodology, Supervision, Writing – review & editing.

Y. Wang and Z. Wu contributed equally to this work.

Funding statement

The authors disclose receipt of the following financial or material support for the research, authorship, and/or publication of this article: this work was supported by the National Natural Science

Foundation of China (Grant No., 81472139) and the Beijing Municipal Health Commission (Grant Nos., BMHC-2019-9 and BMHC-2021-6).

ICMJE COI statement

All authors report grants for this study from the National Natural Science Foundation of China (Grant No. 81472139) and the Beijing Municipal Health Commission (Grant No. BMHC-2019-9 and BMHC-2021-6). C. Wu, Y. Wang, and Z. Wu also report a patent (ZL 2021 1 1402576.7) related to this study.

Data sharing

The data that support the findings for this study are available to other researchers from the corresponding author upon reasonable request.

Ethical review statement

All animal experiments were approved by the Beijing Jishuitan Hospital Animal Care and Use Committee, Beijing, China and performed in accordance with the institutional guidelines for care and use of animals.

Open access funding

This work was supported by the National Natural Science Foundation of China (Grant No., 81472139) and the Beijing Municipal Health Commission (Grant Nos., BMHC-2019-9 and BMHC-2021-6).

© 2024 Wu et al. This is an open-access article distributed under the terms of the Creative Commons Attribution Non-Commercial No Derivatives (CC BY-NC-ND 4.0) licence, which permits the copying and redistribution of the work only, and provided the original author and source are credited. See <https://creativecommons.org/licenses/by-nc-nd/4.0/>